Quasifission and fission rates and their lifetimes in asymmetric reactions forming ^{216}Ra within a dinuclear system approach

M. Varasteh Khanlari* and S. Soheyli
Department of Physics, Bu-Ali Sina University, Post Code 6517433391, Hamedan, Iran
(Received 5 October 2016; revised manuscript received 13 December 2016; published 27 February 2017)

Background: The study of evolution of asymmetric dinuclear systems (DNSs) formed in heavy ion collisions is a topic of intense research. The DNS evolution leads to a variety of reaction channels such as deep inelastic, complete fusion, quasifission, fast fission, fusion-fission, and evaporation of particles. The time evolution of the DNS in the quasifission process and the role of relevant parameters are still not fully understood.
Purpose: The influence of the entrance channel mass asymmetry on the time evolution of an excited and rotating DNS, populated via four reactions with different entrance channel mass asymmetry parameters which all lead to the compound nucleus ^{216}Ra, is explored.
Method: The driving potential, emission barriers for the binary decay (namely the quasifission and intrinsic fusion barriers), rate of the quasifission channel, and the lifetime of an excited DNS, as well as the fission rate and fission lifetime of the compound nucleus ^{216}Ra formed in the ^{12}C + ^{204}Pb, ^{19}F + ^{197}Au, ^{30}Si + ^{186}W, and ^{48}Ca + ^{168}Er reactions, are calculated by the dinuclear system approach.
Results: Our results show that the intrinsic fusion barrier values are equal to zero for the ^{12}C + ^{204}Pb and ^{19}F + ^{197}Au reactions. Therefore, the quasifission signature is extremely hindered for these reactions, while the ^{30}Si + ^{186}W and ^{48}Ca + ^{168}Er calculated results contain quasifission contributions. Provided the quasifission rate is nonzero, the quasifission rate increases with increasing orbital angular momentum ℓ of the composite system for a given excitation energy E^*_{CN} of the compound nucleus. On the other hand, the quasifission lifetime decreases moderately with increasing ℓ. Furthermore, both quasifission and fission rates increase with increasing excitation energy E^*_{CN}, while the quasifission and fission lifetimes decrease with increasing E^*_{CN} for a given ℓ.
Conclusions: Although these reactions with different entrance channels populate the same compound nucleus ^{216}Ra at similar excitation energies, the fused system presents different behaviors for different entrance channel mass asymmetry parameters. In the ^{30}Si + ^{186}W and ^{48}Ca + ^{168}Er reactions having smaller entrance channel mass asymmetry, the quasifission signature dominates over the complete fusion process. Because of the small quasifission barrier for these reactions, the lifetime of the DNS is short and its $E^*_{\rm DNS}$ excitation energy is not sufficient to overcome the saddle point along the way to fusion. Instead, in the ^{12}C + ^{204}Pb and ^{19}F + ^{197}Au reaction systems, at $E^*_{\rm DNS}$ excitation energy higher than the threshold energy, the DNS has sufficient energy and time to reach a compound nucleus. In other words, the model calculations predict that the quasifission rate is negligible for the reactions with higher entrance channel mass asymmetry and complete fusion is a dominant decay channel.

DOI: 10.1103/PhysRevC.95.024617

I. INTRODUCTION

The study of dynamics of massive nuclei collisions near Coulomb barrier energies manifests that the complete fusion of reactants does not take place immediately upon contact of nuclei. In heavy ion reactions, the complete fusion process is strongly hindered by deep inelastic, quasifission, and fast fission processes. These processes cause the appearance of measured fission-like fragments similar to the ones due to the fusion-fission process. The fission-like fragments of quasifission are the main hindrance to the evolution of the dinuclear system (DNS) and formation of the compound nucleus (CN) in these heavy systems. Therefore, the formation of superheavy nuclei is hindered by the quasifission process as the primary reaction mechanism. This process takes place when the DNS tends to break down into two fragments after multinucleon transfer without reaching the stage of a fully equilibrated CN formation. The increase in the sum of the Coulomb interaction and rotational energies in the entrance channel leads to an increase in the number of events going to quasifission. The quasifission products may have characteristics similar to the ones of fusion-fission, such as the total kinetic energy of the fragments, their mass (charge), and angular distributions. The onset of the quasifission signature for very heavy systems having Coulomb factor $Z_P Z_T > 1600$ (where Z_T and Z_P are the target and projectile atomic numbers, respectively) is predicted by an earlier dynamical model [1–3]. However, the existence of the quasifission event has recently been demonstrated in many asymmetric reactions using deformed targets at sub and near Coulomb barrier energies, even though the $Z_P Z_T$ values were lower than 1600 [4–6].

The interaction time (lifetime) of the excited DNS is one of the most important characteristics of the process being considered. Thus, the measurement of lifetimes can give a definitive signature of the nuclear reaction processes. The parameters of the fissioning nucleus such as the fissility, excitation energy, and the angular momentum of the system play a crucial role in the lifetime of the decay process. As the value of each of these parameters increases, the stability of the

*Corresponding author: v.khanlari@gmail.com

nucleus against decay decreases. Quasifission has generally been understood to take place on short time scales around 10^{-20} s [7], while fusion-fission typically occurs on longer time scales, from almost 10^{-20} to 10^{-16} s.

Three main methods are applied to determine the nuclear interaction time scales. The first method, the neutron clock method [8], counts the number of neutrons emitted from an excited DNS before it breaks up into two fragments (pre-scission). The number of emitted pre-scission neutrons increases with increasing lifetime of the nuclear system. In principle, it is sensitive to the time scales of the order of 10^{-22}–10^{-16} s. The second method uses the mass and/or charge distributions of the reaction products together with the angular distributions to estimate the interaction time of the DNS [7,9]. It can provide an almost model-independent estimate of quasifission time scales. Interaction times below 10^{-20} s were deduced by this method. The third method is the crystal blocking method. The angular distribution of the reaction fragments with respect to a major crystal axis of the target is measured by this method [10]. Fission fragments emitted in this direction are deflected away by the row of atoms, unless the formed CN has recoiled far enough from the lattice site. This method is sensitive to longer time scales, in the range 10^{-18} to 10^{-16} s [11]. It is thus sensitive to the time scales associated with the fusion-fission, and can indicate the appearance of the fusion-fission between the predominant quasifission events [12]. The crystal blocking method has recently been applied to fission-like events in reactions producing superheavy nuclei [11–13].

The quasifission probability should increase with increasing charges of both the projectile and dinucleus. Since the time scale of the quasifission is expected to be shorter than for that of fusion-fission, the mean quasifission time should decrease with increasing charge numbers of the projectile and dinucleus.

Lifetime of the DNS is strongly influenced by the charge numbers of projectile and target nuclei, beam energy, and angular momentum, which determine the depth of the minimum (pocket) in the nucleus-nucleus potential well. The lifetime of the DNS should be enough for its transformation into a CN (complete fusion of interacting nuclei). In general, the mean lifetime of the DNS is correlated with the number of transferred nucleons and the energy dissipation which characterize the exit channel, namely the mass, charge, and angular distributions, and the total kinetic energy of the reaction products.

The main scope of this work is to determine the driving potential, the quasifission B_{qf} and intrinsic fusion $B^*_{\rm fus}$ barriers, rate of the quasifission channel, and lifetime of an excited DNS for the ^{12}C + ^{204}Pb, ^{19}F + ^{197}Au, ^{30}Si + ^{186}W, and ^{48}Ca + ^{168}Er reactions leading to the same compound nucleus ^{216}Ra. The fission rate and the time scale of the fission are also determined for the ^{48}Ca + ^{168}Er reaction. The calculations were carried out within the combined dynamical-statistical model based on the dinuclear system (DNS). These calculations are the first performed by the DNS approach. We have already estimated the internuclear potential energy, complete fusion probability, and excitation functions of capture, fusion, and quasifission processes, as well as the relative yield of complete fusion and quasifission components for the above mentioned reactions within the framework of the DNS model [14].

This paper is organized in the following way. The outline of the theoretical method is given in Sec. II. Section III is devoted to our calculated results. The conclusions of this research are presented in Sec. IV.

II. DESCRIPTION OF THE THEORETICAL APPROACH

All heavy ion reaction channels with full momentum transfer at low collision energies, called the capture reaction, occur through the stage of dinuclear system (DNS) formation. The necessary condition of the capture mechanism is overcoming the Coulomb barrier and rotational energy of the entrance channel by sufficient energy of the projectile nucleus in order to trap the DNS in the potential well of the nucleus-nucleus interaction. The DNS consists of two nuclei which touch each other and keep their own individuality [15]. The DNS after the capture mechanism can evolve as the result of the nucleon exchange mechanism between clusters that change the mass and charge asymmetry coordinates.

The nucleus-nucleus interaction potential of the DNS versus the charges Z_1 and Z_2 of the forming dinuclear system and the distance R between their centers is given by [16]

$$\begin{aligned} &V(R,Z_1,Z_2,\ell,\{\beta_i\}) \\ &\quad = V_C(R,Z_1,Z_2,\{\beta_i\}) + V_N(R,Z_1,Z_2,\{\beta_i\}) \\ &\qquad + V^{(\rm DNS)}_{\rm rot}(\ell,\{\beta_i\}), \end{aligned} \tag{1}$$

where V_C, V_N, and $V^{\rm DNS}_{\rm rot}$ are the Coulomb, nuclear, and rotational potentials, respectively; $\beta_{i=1,2}$ are the quadrupole deformation parameters of nuclei forming the DNS.

The evolution of the DNS with the initial charge numbers of projectile and target nuclei (Z_P and Z_T, respectively) to complete fusion is determined by the potential energy surface (PES), $U(A_1,Z_1;R)$. Assuming a small overlap of nuclei in the DNS, $U(A_1,Z_1;R)$ is calculated versus charges Z_1, Z_2 forming the dinuclear system and the distance R between their centers [17]:

$$U(A_1,Z_1;R) = Q - V^{CN}_{\rm rot}(\ell) + V(R,Z_1,Z_2,\ell,\beta_i), \tag{2}$$

$$Q = B_1(Z_1) + B_2(Z_2) - B_{CN}(Z_{CN}), \tag{3}$$

where Q is the reaction energy balance; B_1, B_2, and $B_{CN}(Z_{CN} = Z_1 + Z_2)$ are the binding energies of the fragments in the DNS and of the compound nucleus at their ground states, respectively, which are taken from Ref. [18].

The driving potential $U_{dr}(A_1,Z_1;R_m)$ is extracted from the potential energy surface $U(A_1,Z_1;R)$, where R_m is the internuclear distance corresponding to the minimum of the nucleus-nucleus potential well $V(R)$. Indeed, the nucleus-nucleus potential well has a pocket with a minimum situated for the pole-pole orientation at the distance between the nuclei R_m corresponding to the touching configuration [19]. Further details concerning the theoretical approach can be found in Ref. [14].

The intrinsic fusion barrier $B^*_{\rm fus}$ is a dynamical hindrance in the DNS evolution on the way to form the compound nucleus in the mass asymmetry coordination of the DNS. The barrier $B^*_{\rm fus}$ is determined as the difference between the maximum value of the driving potential between $Z_1 = 0$ and Z_P and its

value corresponding to the initial charge value [20],

$$B^{*}_{\rm fus} = U^{\rm max}_{dr} - U_{dr}(Z_P), \tag{4}$$

where $U^{\rm max}_{dr}$ is the max value of the driving potential between $Z_1 = 0$ and Z_P. The formation of the compound nucleus is hindered if the excitation energy of the DNS is less than the value of $B^{*}_{\rm fus}$.

The decay of the DNS in the relative distance R can be treated using the one-dimensional Kramers rate [21],

$$\Lambda_{qf}(\Theta_{\rm DNS}) = \frac{\omega_m}{2\pi\omega_{qf}}\left(\sqrt{\left(\frac{\Gamma}{2\hbar}\right)^2 + (\omega_{qf})^2} - \frac{\Gamma}{2\hbar}\right) \times \exp\left(-\frac{B_{qf}(Z_1,A_1)}{\Theta_{\rm DNS}(Z_1,A_1)}\right). \tag{5}$$

Obviously this rate falls exponentially with increasing quasifission barrier $B_{qf}(Z_1,A_1)$ [14] for a given charge and mass asymmetry. In this equation, the quantity Γ denotes a double average width of the contributing single-particle states near the Fermi surface and $\Gamma = 2$ MeV [22]; ω_{qf} is the frequency of the inverted harmonic oscillator approximating the interaction potential shape of two nuclei for a given DNS configuration (for a given Z_1 and Z_2) around the top of the quasifission barrier placed at R_{qf}, and ω_m is the frequency of the harmonic oscillator approximating the potential in R on the bottom of its pocket placed at R_m. Therefore,

$$\omega^2_{qf} = \mu^{-1}_{qf}\left|\frac{\partial^2 V(R)}{\partial R^2}\right|_{R=R_{qf}}, \quad \omega^2_m = \mu^{-1}_{qf}\left|\frac{\partial^2 V(R)}{\partial R^2}\right|_{R=R_m}, \tag{6}$$

where, $\mu_{qf} \approx \frac{A_1.A_2}{A}$; A_1 and A_2 are the mass numbers of the quasifission fragments, and $A = A_1 + A_2$ [20]. The local temperature of the DNS over the quasifission barrier is calculated by using the Fermi-gas model as $\Theta = (\frac{E^{*}_{\rm DNS} - B_{qf}}{a})^{1/2}$ corresponding to the local excitation energy $E^{*}_{\rm DNS}$ of the DNS in the entrance channel [23],

$$E^{*}_{\rm DNS} = E_{c.m.} - V(R_m), \tag{7}$$

where $E_{c.m.}$ is the center-of-mass energy. The level density parameter a is also taken from Ref. [24] as $a = 0.134\,A - 1.21 \times 10^{-4}A^2$, found by analyzing the experimental data for heavy nuclei with $Z \leqslant 102$.

For the quite short transient times, the fission rate is defined by its quasistationary value in accordance with the Kramers formula as follows [25]:

$$\Lambda_{\rm fis}(\Theta) = \frac{\omega_{gs}}{2\pi\omega_f}\left(\sqrt{\left(\frac{\Gamma_\circ}{2\hbar}\right)^2 + (\omega_f)^2} - \frac{\Gamma_\circ}{2\hbar}\right) \times \exp\left(-\frac{B_{\rm fis}(Z_1,A_1)}{\Theta(Z_1,A_1)}\right), \tag{8}$$

where ω_{gs} and ω_f are the frequencies of the normal and inverted oscillators that approximate the potential in the ground state and around the top of the fission barrier for a given charge and mass asymmetry, respectively. The values of $\omega_{gs} = \omega_f = 0.5$ MeV and $\Gamma_0 = 2$ MeV are used in our calculations.

The fission barrier is given by the following relation [26]:

$$B_{\rm fis}(\ell,\Theta) = cB^{m}_{\rm fis}(\ell) - h(\Theta)q(\ell)\partial W, \tag{9}$$

where $B^{m}_{\rm fis}(\ell)$ is the macroscopic part of fission barrier. This quantity depends on the angular momentum ℓ and it is parametrized by Sierk according to the rotating finite range model [27]. The microscopic part of the fission barrier including shell correction $\partial W = \partial W_{\rm sad} - \partial W_{gs} \cong -\partial W_{gs}$ is taken from Ref. [28]. The damping of the microscopic fission barrier on the excitation energy and angular momentum of a fissioning nucleus is taken into account by the following relations [26]:

$$h(\Theta) = \{1 + \exp[(\Theta - \Theta_\circ)/d]\}^{-1}, \tag{10}$$

$$q(\ell) = \{1 + \exp[(\ell - \ell_{1/2})/\Delta(\ell)]\}^{-1}. \tag{11}$$

The constants for the macroscopic fission barrier scaling, temperature, and angular momentum dependencies of the microscopic correction are chosen as $c = 1.0$, $d = 0.3$ MeV, $\ell_{1/2} = 20\hbar$ for nuclei with $Z \simeq 80$–100, and $\Delta(\ell) = 3\hbar$ [20].

In Eq. (10), $\Theta_\circ = 1.16$ MeV and $\Theta = \sqrt{\frac{E^{*}_{CN}(\ell)}{a}}$ represents the nuclear temperature depending on the level density parameter a and the excitation energy $E^{*}_{CN}(\ell)$ of the compound nucleus; $E^{*}_{CN}(\ell) = E_{c.m.} + Q - V^{CN}_{\rm rot}(\ell)$ [19].

III. RESULTS AND DISCUSSION

The present paper is devoted to investigating the ^{12}C + ^{204}Pb, ^{19}F + ^{197}Au, ^{30}Si + ^{186}W, and ^{48}Ca + ^{168}Er asymmetric reactions which all lead to the ^{216}Ra compound nucleus. Our treatment is based on the dinuclear system (DNS) approach. This interpretation assumes that the DNS forms after the colliding nuclei pass over the Coulomb barrier and come to a touching configuration. In the DNS approach, the potential energy has an important role and depends on the masses of the products in the quasifission process. In Fig. 1, the driving potential $U_{dr}(Z_1)$ extracted from the potential energy surface $U(A_1, Z_1; R)$ for the different entrance channels leading to the

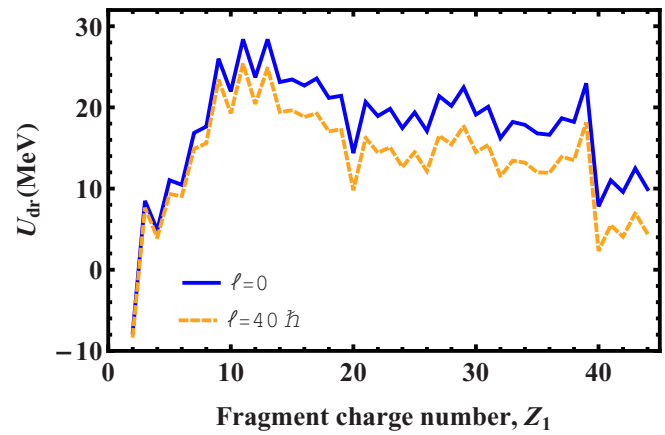

FIG. 1. The driving potential $U_{dr}(Z_1)$ calculated for $\ell = 0\hbar$ and $40\hbar$ for the DNS formed in the reactions leading to the formation of the same compound nucleus ^{216}Ra versus the charge number of the lighter fragment of the DNS based on the DNS approach.

formation of the ^{216}Ra nucleus is presented for the given values of the orbital angular momentum $\ell = 0\hbar$ and $40\hbar$ as the blue solid line and orange dashed line, respectively.

Our calculations indicate that the driving potential depends strongly on the charge asymmetry of the DNS constituents. It is observed that the maximum value of the driving potential obtains at $Z = 11$ for the studied reactions.

A. The intrinsic fusion barrier $B^*_{\rm fus}$

In the DNS model, the fusion process is considered, as the diffusion process occurred as a result of the transfer of nucleons from the light nucleus to the heavy one. The dynamical hindrance in the DNS evolution on the way to complete fusion is the intrinsic fusion barrier $B^*_{\rm fus}$ in the mass asymmetry coordination of the DNS.

The variations of $B^*_{\rm fus}$ as a function of the charge Z_1 of the lighter fragment of the DNS for the composite system ^{216}Ra and also for $\ell = 0\hbar$, $30\hbar$, and $50\hbar$ (dashed green, dot-dashed orange, and solid red lines, respectively) are shown in Fig. 2(a). It is manifested that $B^*_{\rm fus}$ increases by increasing the orbital angular momentum ℓ. In general, the fusion barrier $B^*_{\rm fus}$ for the DNS increases by decreasing the charge asymmetry parameter in the initial DNS [29].

In Fig. 2(b), the general behavior of the intrinsic fusion barriers $B^*_{\rm fus}$ versus the angular momentum ℓ for the ^{30}Si $+^{186}$W and ^{48}Ca $+^{168}$Er reactions at $E^*_{CN} = 60$ MeV are represented as the dot-dashed green and dot-dashed orange curves (curves from bottom to top), respectively. These curves are plotted up to the maximum value of angular momentum ℓ_m for each reaction at the given excitation energy of the compound nucleus. It should be noted that the $B^*_{\rm fus}$ values are equal to zero for the two ^{12}C $+^{204}$Pb and ^{19}F $+^{197}$Au reaction systems.

The values of $B^*_{\rm fus}$ change slowly when ℓ varies in the interval $0\hbar$ to $25\hbar$ due to the larger value of the moment of inertia in the massive nuclei reactions. For heavier systems, the variations of $B^*_{\rm fus}$ are even smaller.

The general behaviors of $B^*_{\rm fus}$ versus the charge number of the lighter fragment Z_1 in the DNS and the angular momentum ℓ are also shown in Fig. 2(c). The red broken line corresponds to a cut of the intrinsic fusion barrier $B^*_{\rm fus}$ at $\ell = 50\hbar$, and the dashed dark orange curve corresponds to a cut of the intrinsic fusion barrier $B^*_{\rm fus}$ at $Z_1 = 20$.

B. The quasifission barrier B_{qf}

The evolution of the DNS by nucleon exchange at the minimum position of the interaction potential well after the capture mechanism of the colliding system along the relative distance R between the interacting nuclei will lead to quasifission of the DNS. In order for the DNS to undergo decay in two fragments (the quasifission process), it is necessary to overcome the quasifission barrier B_{qf}. This barrier, which keeps the DNS nuclei in contact, measures the depth of the interaction potential pocket situated at the distance R_m. Thus, the stability of the DNS against the quasifission process

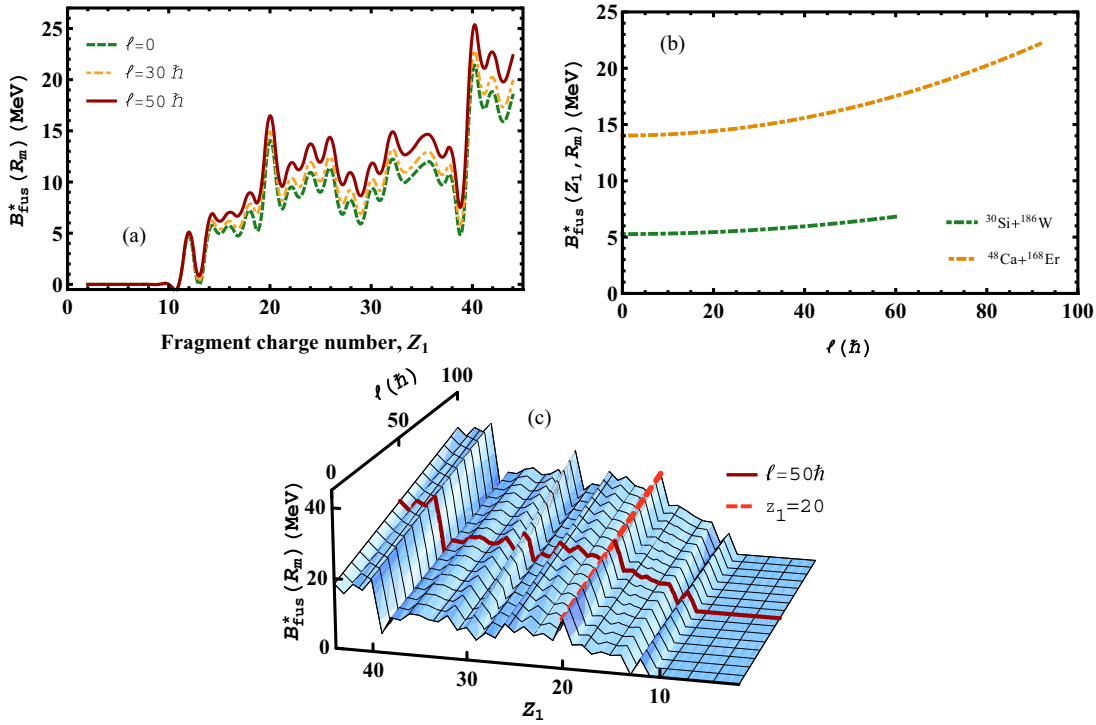

FIG. 2. (a) The intrinsic fusion barrier $B^*_{\rm fus}$ predicted for the DNS formed in the reactions leading to the compound nucleus ^{216}Ra as a function of the charge Z_1 of the lighter fragment of the DNS for three different values of the angular momentum, $\ell = 0\hbar$, $30\hbar$, and $50\hbar$, respectively, based on the DNS model. (b) The behavior of the intrinsic fusion barrier $B^*_{\rm fus}$ versus ℓ is plotted for the ^{30}Si $+^{186}$W and ^{48}Ca $+^{168}$Er reactions at $E^*_{CN} = 60$ MeV. (c) The intrinsic fusion barrier $B^*_{\rm fus}$ predicted for the DNS formed in the reactions leading to the compound nucleus ^{216}Ra as a function of the Z_1 and ℓ values.

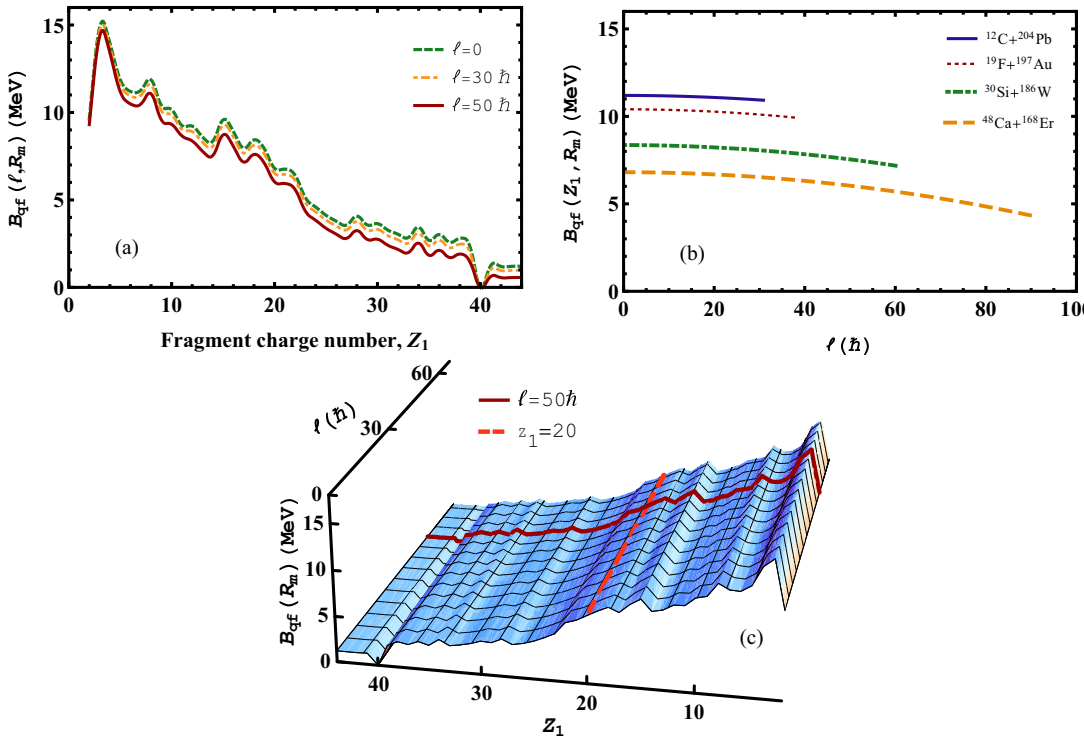

FIG. 3. (a) The quasifission barrier B_{qf} predicted for the DNS formed in the reactions leading to the compound nucleus ^{216}Ra as a function of the charge Z_1 of the lighter fragment of the DNS for three different values of the angular momentum, $\ell = 0\hbar$, $30\hbar$, and $50\hbar$, respectively, based on the DNS model. (b) The behavior of the quasifission barrier B^*_{qf} versus ℓ for the studied reactions at $E^*_{CN} = 60$ MeV. (c) The quasifission barrier B^*_{qf} predicted for the DNS formed in the reactions leading to the compound nucleus ^{216}Ra as a function of the Z_1 and ℓ values.

is determined by the depth B_{qf} of the potential well. The dominant role of the quasifission channel in reactions with massive nuclei leads to strong hindrance to the formation of a CN during the evolution of the DNS.

The behavior of B_{qf} versus the charge Z_1 of the lighter fragment of the DNS for the composite system ^{216}Ra at the given values of $\ell = 0\hbar$, $30\hbar$, and $50\hbar$ is shown in Fig. 3(a). The dashed green, dot-dashed orange, and solid red lines (curves from top to bottom) correspond to the quasifission barrier at $\ell = 0\hbar$, $30\hbar$, and $50\hbar$, respectively. The variations of the quasifission barrier B_{qf} against ℓ in the ^{12}C + ^{204}Pb, ^{19}F + ^{197}Au, ^{30}Si + ^{186}W, and ^{48}Ca + ^{168}Er reactions, which all lead to the ^{216}Ra compound nucleus at $E^*_{CN} = 60$ MeV, are represented as the solid blue, dotted red, dot-dashed green, and dashed orange curves, respectively (curves from top to bottom) in Fig. 3(b). The values of B_{qf} are estimated up to the maximum value of angular momentum ℓ_m for each reaction at the given excitation energy of the compound nucleus. It is seen that the values of B_{qf} change slowly when ℓ increases around from $0\hbar$ to $25\hbar$ due to the larger value of the moment of inertia in massive nuclei reactions. Figure 3(c) indicates the dependence of B_{qf} on the charge value Z_1 and ℓ. In this figure, the red line is related to a cut of the quasifission barrier B_{qf} at $\ell = 50\hbar$, and the dashed dark orange curve corresponds to the behavior of the B_{qf} versus ℓ at $Z_1 = 20$.

It is concluded that the depth B_{qf} of the potential pocket decreases with increasing ℓ due to the growth of the repulsive centrifugal part in Eq. (1) [30]. Therefore, the contribution of the quasifission channel increases with increasing ℓ and also the values of B_{qf} decrease monotonically with increasing Z_1. Note that increasing the entrance barrier leads to very shallow pockets in the nucleus-nucleus potential for near symmetric configurations. On the other hand, the quasifission barriers providing the relative stability of the DNS formed via the ^{12}C + ^{204}Pb and ^{19}F + ^{197}Au channels are greater than those obtained for the ^{30}Si + ^{186}W and ^{48}Ca + ^{168}Er reactions.

C. The quasifission rate and lifetime of an excited DNS

The decay of the DNS is given by the following decay law:

$$\frac{dN}{dt} = -\Lambda_{qf} N, \tag{12}$$

where Λ_{qf} is the quasifission decay constant, N denotes the number of nuclei that have not undergone quasifission at the time t, and dN is the number of nuclei that have escaped within the time interval t to $t + dt$.

The mean lifetime of an excited DNS, $\tau_{\rm DNS}$, is also expressed as

$$\tau_{\rm DNS} = \frac{1}{\Lambda_{qf}}. \tag{13}$$

The values of the quasifission barrier B_{qf}, which depend on the charge value Z_1, are mainly responsible for the lifetime of the DNS. During this time, the DNS evolves in the charge (mass) asymmetry degrees of freedom with exchange of nucleons between the constituents of the dinuclear system.

TABLE I. The values of $\hbar\omega_m$ and $\hbar\omega_{qf}$ for the studied reactions leading to the ^{216}Ra compound nucleus.

Reaction	$\hbar\omega_m$ (MeV)	$\hbar\omega_{qf}$ (MeV)
$^{12}C+^{204}Pb$	0.57	0.36
$^{19}F+^{197}Au$	6.01	3.92
$^{30}Si+^{186}W$	4.78	3.23
$^{48}Ca+^{168}Er$	4.15	2.75

The DNS lifetime may be not sufficient to transform into a compound nucleus and so the quasifission process takes place. Therefore, the lifetime of a partially equilibrated dinuclear complex should be shorter than that of a fully equilibrated compound nucleus.

In this research, the quasifission rate and the mean lifetime of an excited DNS for the $^{12}C+^{204}Pb$, $^{19}F+^{197}Au$, $^{30}Si+^{186}W$, and $^{48}Ca+^{168}Er$ asymmetric reactions which all lead to the ^{216}Ra compound nucleus are estimated by using Eqs. (5) and (13), respectively. Using the DNS model, the values of $\hbar\omega_m$ and $\hbar\omega_{qf}$ for the above reactions are predicted and the results are listed in Table I.

The behaviors of the quasifission rate and the mean lifetime of an excited DNS versus the orbital angular momentum ℓ for the different entrance channels and for several excitation energies are plotted in Figs. 4 and 5, respectively.

It must be stressed that both the quasifission barrier B_{qf} and the nuclear temperature Θ_{DNS} decrease with increasing angular momentum ℓ. Our results show that the values of quasifission rate Λ_{qf} change weakly when ℓ increases around from $0\hbar$ to $25\hbar$ due to very weak dependence of the B_{qf} values on angular momentum in this interval. However, for the higher values of ℓ ($\ell > 25\hbar$), two different behaviors are observed: for smaller values of E^*_{CN}, the reduction of the quasifission barrier B_{qf} is slower than the reduction of the temperature Θ_{DNS} with increasing ℓ due to the decrease of Λ_{qf}. On the other hand, at larger excitation energies E^*_{CN}, the quasifission barrier B_{qf} decreases faster than the temperature Θ_{DNS} with increasing ℓ. Therefore, the quasifission rate Λ_{qf} increases moderately with increasing ℓ. In particular, this behavior is obviously seen for the reaction systems induced by the ^{30}Si and ^{48}Ca projectiles.

As shown in Fig. 5, the values of DNS lifetime τ_{DNS} are nearly constant when ℓ varies in the interval $0\hbar$ to $25\hbar$ due to very weak dependency of the values of B_{qf} on ℓ in this interval. However, for higher values of ℓ ($\ell > 25\hbar$), similar to the quasifission rate Λ_{qf}, the DNS lifetime presents two different behaviors: for smaller values of E^*_{CN}, the reduction of the quasifission rate Λ_{qf} with increasing ℓ leads to increasing τ_{DNS}. On the other hand, at larger excitation energies E^*_{CN}, the growth of the quasifission rate Λ_{qf} with increasing ℓ leads to the reduction of the stability of the DNSs formed in the $^{30}Si+^{186}W$ and $^{48}Ca+^{168}Er$ reactions.

The behaviors of Λ_{qf} and τ_{DNS} versus ℓ for the studied reactions are plotted up to the maximum values of angular momentum l_m leading to the capture mechanism for the reactions at given beam energies. The maximum values of ℓ_m for the $^{12}C+^{204}Pb$, $^{19}F+^{197}Au$, $^{30}Si+^{186}W$, and $^{48}Ca+^{168}Er$ reactions as a function of the excitation energy E^*_{CN} are predicted with the help of Refs. [19,31], and the results are reported in Fig. 6.

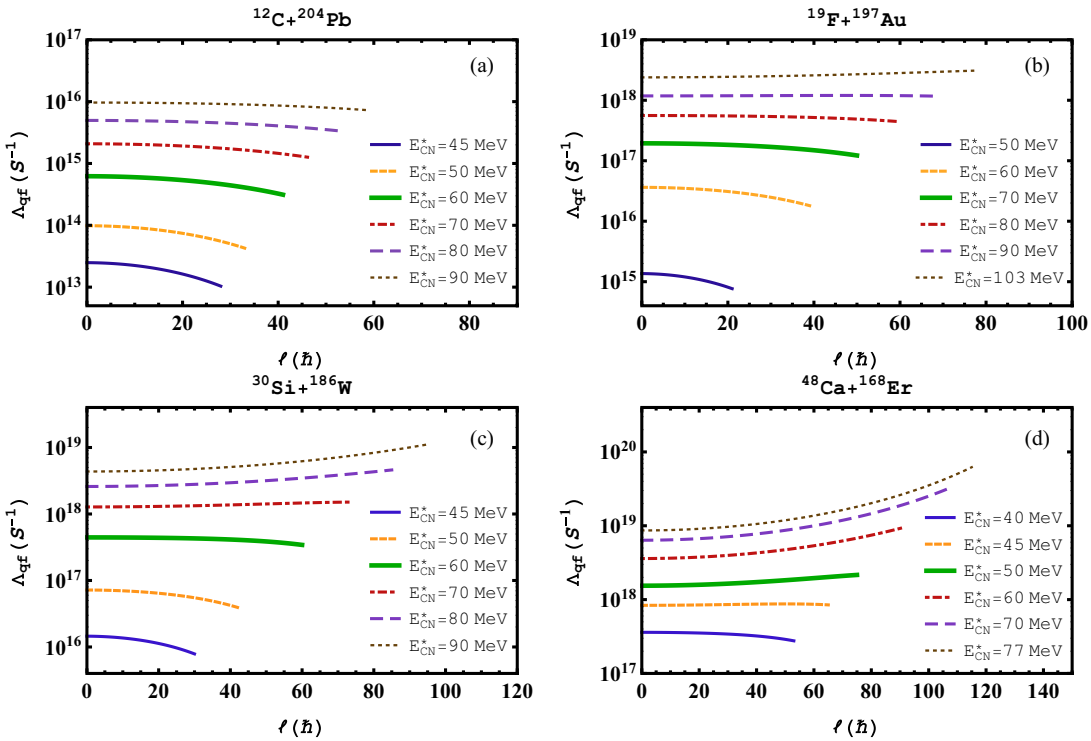

FIG. 4. The dependence of the quasifission rate Λ_{qf} of the DNS decay versus the angular momentum ℓ within the framework of the DNS model for the $^{12}C+^{204}Pb$, $^{19}F+^{197}Au$, $^{30}Si+^{186}W$, and $^{48}Ca+^{168}Er$ asymmetric reactions are reported in (a), (b), (c), and (d), respectively.

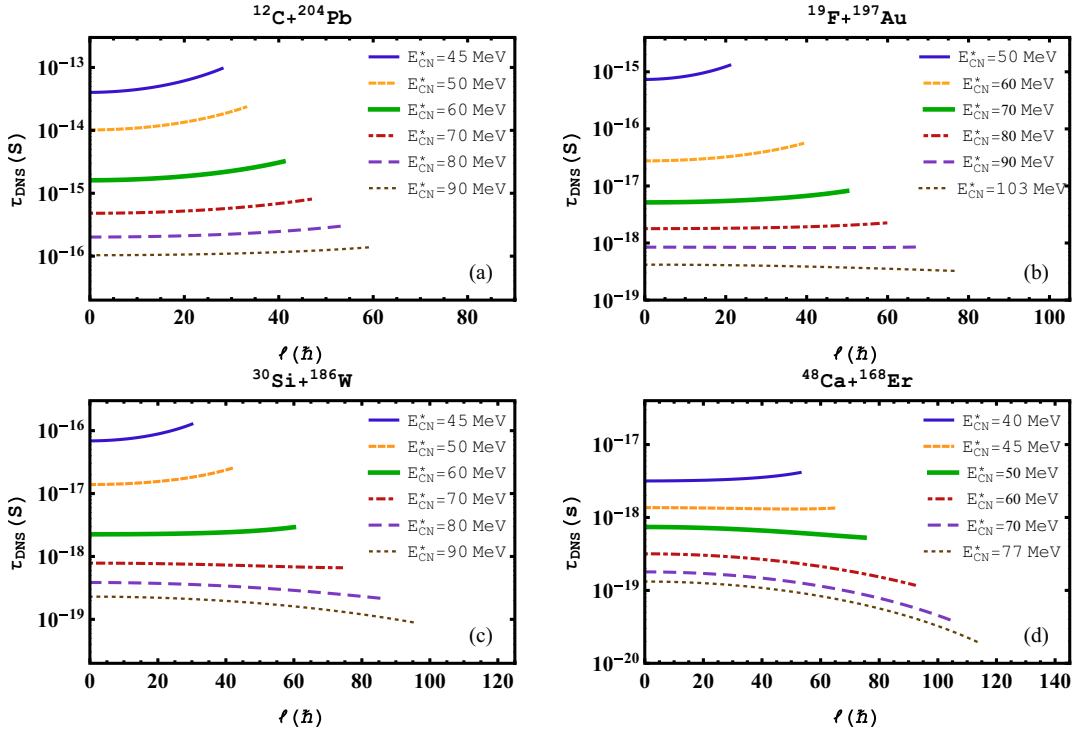

FIG. 5. The behavior of the lifetime τ_{DNS} of the excited DNS versus the angular momentum ℓ within the framework of the DNS model for the $^{12}C+^{204}Pb$, $^{19}F+^{197}Au$, $^{30}Si+^{186}W$, and $^{48}Ca+^{168}Er$ asymmetric reactions are shown in (a), (b), (c), and (d), respectively.

It is seen that the maximum values of angular momentum ℓ_m for the four investigated reactions are in the range of about 50$\hbar$ and 100$\hbar$ at excitation energies within the interval of 80–100 MeV, while the capture cross sections of these reactions have about the same values of 1000 mb [14]. Such behaviors are connected with partial cross sections, as well as can be explained by those partial capture cross sections that are determined by the angular momentum ℓ, center-of-mass energy of the system, and transmission probability. The transmission probability is around 1 for the studied reactions at excitation energies within the interval of 80–100 MeV. Therefore, the DNS model predicts the same values of the capture cross section for the $^{12}C+^{204}Pb$, $^{19}F+^{197}Au$, $^{30}Si+^{186}W$, and $^{48}Ca+^{168}Er$ reactions at a given excitation energy.

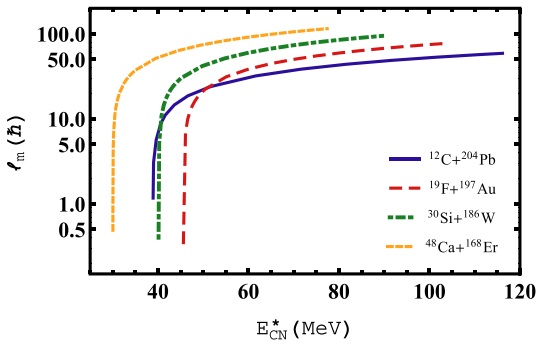

FIG. 6. The behavior of the maximum values of angular momentum ℓ_m for the reactions leading to the formation of the same compound nucleus ^{216}Ra versus the excitation energy E^*_{CN}.

The behaviors of the quasifission rate and the mean lifetime of an excited DNS with the excitation energy at fixed values of the orbital angular momentum ℓ for the different entrance channels are plotted in Figs. 7 and 8, respectively. These curves are plotted up to the beam energies at which the angular momentum ℓ of the DNS is equal to the maximum value of angular momentum ℓ_m.

It can be concluded that the quasifission rate increases with increasing excitation energy E^*_{CN} at the same values of the angular momentum ℓ. Furthermore, it should be noted that the rate Λ_{qf} decreases with increasing ℓ for smaller values of E^*_{CN}. On the other hand, at larger excitation energies E^*_{CN}, the quasifission rates of the $^{30}Si+^{186}W$ and $^{48}Ca+^{168}Er$ reactions increase with increasing ℓ.

Our results indicate that the mean lifetime of an excited DNS decreases with increasing excitation energy E^*_{CN} and it also increases with increasing ℓ for small values of E^*_{CN}. At larger excitation energies, the survival probability of the DNS formed through the reactions induced by the ^{30}Si and ^{48}Ca beams also decreases with increasing ℓ.

In order to investigate the dependence of the quasifission rate Λ_{qf} on the charge Z_1 of the lighter fragment in the DNS, the values of Λ_{qf} for all populated DNS configurations within the framework of the DNS model are estimated according to Eq. (5). The obtained results are presented in Fig. 9(a) at the given quantities of $E^*_{CN} = 60$ MeV and $\ell = 30\hbar$. It is seen that the quasifission rate (dots) increases strongly for the most symmetric combinations. Therefore, it can be observed that,

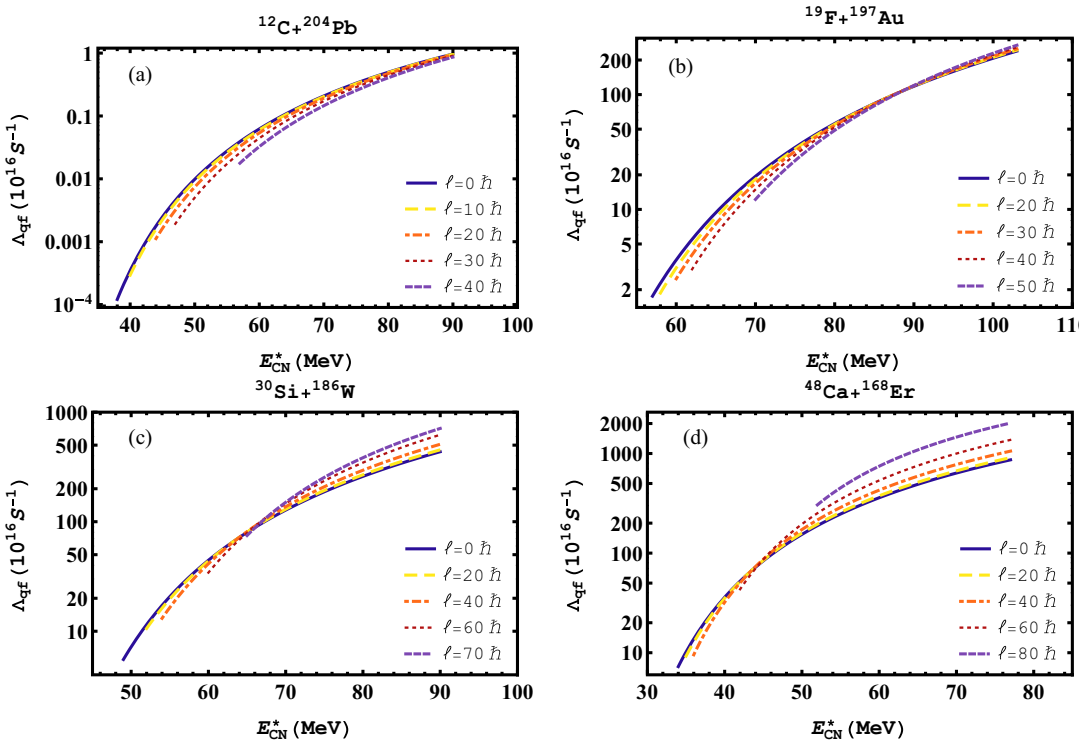

FIG. 7. The dependence of the DNS decay rate Λ_{qf} versus the excitation energy E^*_{CN} for the DNSs formed in the $^{12}C+^{204}Pb$, $^{19}F+^{197}Au$, $^{30}Si+^{186}W$, and $^{48}Ca+^{168}Er$ reactions are shown in (a), (b), (c), and (d), respectively.

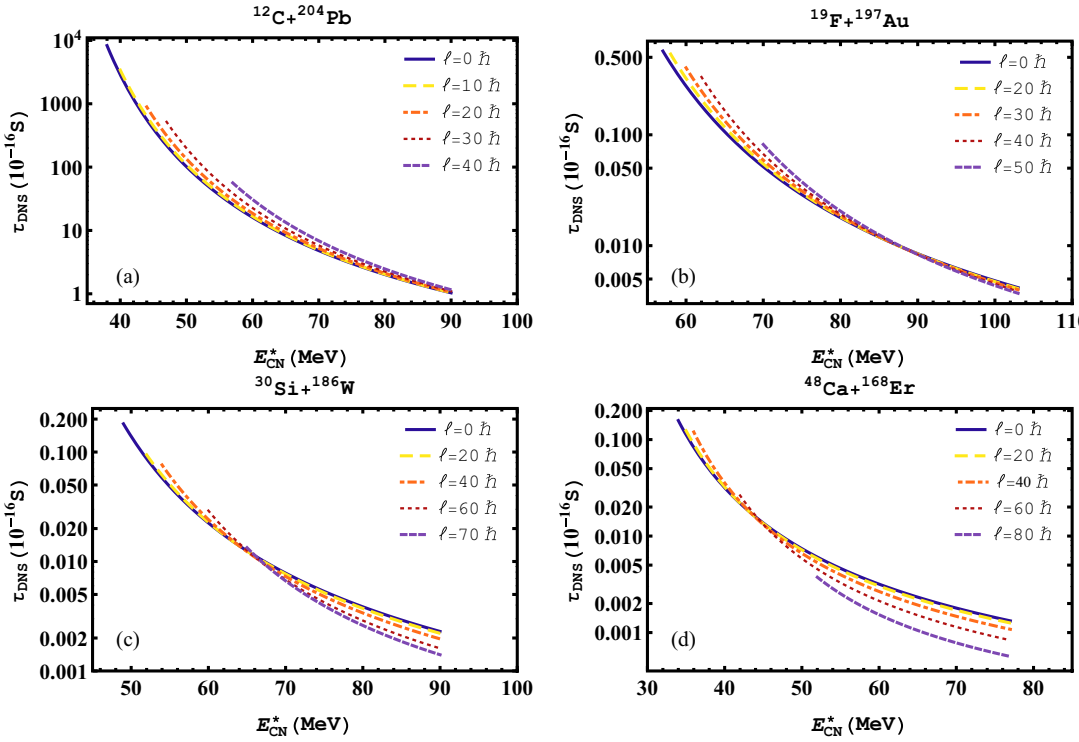

FIG. 8. The behavior of the lifetime τ_{DNS} of the excited DNS formed via the different entrance channels versus the excitation energy E^*_{CN} at the given angular momentum ℓ within the framework of the DNS approach.

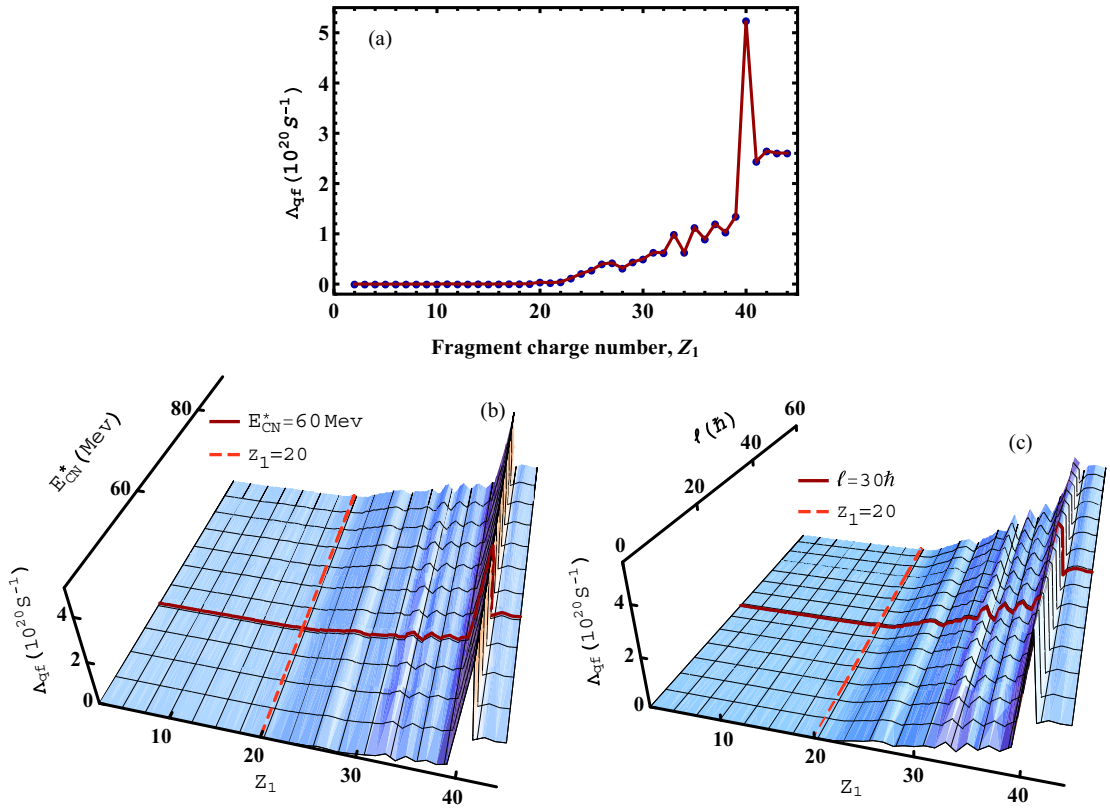

FIG. 9. (a) The calculated (dots) quasifission rate Λ_{qf} for the DNS formed in the reactions forming the compound nucleus ^{216}Ra as a function of the charge Z_1 of the lighter fragment in the DNS within the DNS model at the excitation energy $E^*_{CN} = 60$ MeV and at the angular momentum $\ell = 30\hbar$. (b) Obtained results for Λ_{qf} against Z_1 and E^*_{CN}. (c) The behavior of Λ_{qf} versus Z_1 and ℓ.

for the reactions having larger entrance channel asymmetry and deeper interaction potential pocket, the dominant event during the DNS evolution is complete fusion. Moreover, one can stress that the quasifission barrier B_{qf} plays a crucial role in the complete fusion features that depend heavily on the charge and angular momentum of the DNS.

The general trend of Λ_{qf} versus the charge value Z_1 and the excitation energy E^*_{CN}, as well as its behavior versus the charge value Z_1 and the angular momentum ℓ, are shown in Figs. 9(b) and 9(c), respectively. In these figures, the red broken lines correspond to the variations of Λ_{qf} at $E^*_{CN} = 60$ MeV and $\ell = 30\hbar$, and the dashed dark orange curves are related to the variations of Λ_{qf} in terms of E^*_{CN} and ℓ for a given value of $Z_1 = 20$.

The charge asymmetry η_Z, quasifission barrier B_{qf}, and lifetime $\tau_{\rm DNS}$ of an excited DNS for four different channels leading to the DNS corresponding to the ^{216}Ra compound nucleus are calculated at $E^*_{CN} = 60$ MeV and $\ell = 30\hbar$. The results are listed in Table II.

The results for the reactions induced by heavy ions such as ^{30}Si and ^{48}Ca projectiles show that the quasifission process dominates during the evolution of the DNS, so that the lifetimes $\tau_{\rm DNS}$ of these reactions are smaller than those of reactions with larger entrance channel charge asymmetry induced by the ^{12}C and ^{19}F ions. Therefore, the DNSs formed in the ^{30}Si + ^{186}W and ^{48}Ca + ^{168}Er reactions tend to break down into two fragments, bypassing the stage of the formation of a fully equilibrated compound nucleus. On the other hand, fused dinuclear systems with larger entrance channel charge asymmetry (such as the reactions induced by ^{12}C and ^{19}F ions) have larger B_{qf} quasifission barriers and sufficient lifetimes, so they may tend to transform into fully equilibrated compound nuclei. In these reactions, the quasifission signature is extremely hindered.

D. The fission rate and the fission time scale

Fission is a dynamical process for which a nucleus needs the time to deform up to the scission point. The time scale of an induced fission process is an interesting topic from the experimental and theoretical points of view. Knowledge of the lifetime is crucial for the understanding of the nuclear reaction processes. The total time involved in a fission process can be schematically divided in two main components. The first

TABLE II. Charge asymmetry, quasifission barrier B_{qf}, and lifetime $\tau_{\rm DNS}$ for the studied reactions leading to ^{216}Ra.

Reaction	η_z	B_{qf} (MeV)	$\tau_{\rm DNS}$ (s)
^{12}C + ^{204}Pb	0.86	12.93	2.26×10^{-15}
^{19}F + ^{197}Au	0.80	10.11	4.02×10^{-17}
^{30}Si + ^{186}W	0.68	8.06	2.33×10^{-18}
^{48}Ca + ^{168}Er	0.55	6.53	2.52×10^{-19}

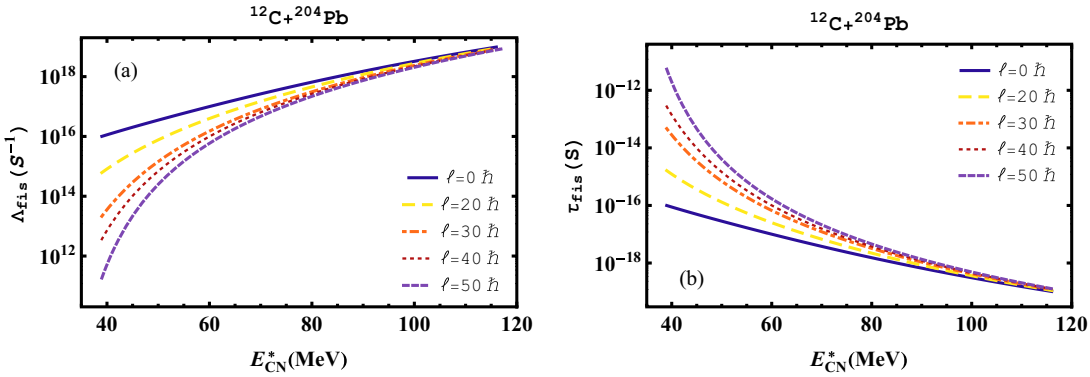

FIG. 10. The fission rate $\Lambda_{\rm fis}$ (curves from top to bottom) and the fission lifetime $\tau_{\rm fis}$ (curves from bottom to top)for the $^{12}C+^{204}Pb$ reaction are calculated within the framework of the DNS model versus the excitation energy E^*_{CN} at the same values of angular momentum ℓ in (a) and (b), respectively.

component corresponds to the time needed for the nucleus to pass over the saddle point. The second component corresponds to the deformation time from the saddle point up to the scission point.

The fission rate $\Lambda_{\rm fis}$ and fission lifetime $\tau_{\rm fis}$ for the most asymmetric $^{12}C+^{204}Pb$ and almost symmetric $^{48}Ca+^{168}Er$ reactions are calculated. The variations of the fission rate $\Lambda_{\rm fis}$ (curves from top to bottom), as well as the fission lifetime $\tau_{\rm fis}$ (curves from bottom to top), in terms of E^*_{CN} at the same values of the orbital angular momentum ℓ for the two above reactions are plotted in Figs. 10(a) and 10(b) and in Figs. 11(a) and 11(b), respectively.

It is observed that the fission rate $\Lambda_{\rm fis}$ increases by increasing the excitation energy E^*_{CN}. Unlike the fission rate, the fission time $\tau_{\rm fis}$ generally decreases by increasing the excitation energy E^*_{CN}. Therefore, the stability of the massive compound nucleus decreases due to the reduction of the fission barrier by increasing its excitation energy.

IV. CONCLUSIONS

The theoretical method based on the dinuclear system (DNS) approach, with the double-folding formation for the nuclear part of the nucleon-nucleon potential at the pole-pole orientation, is applied in order to analyze the reactions leading to the formation of the compound nucleus ^{216}Ra at similar excitation energies. The driving potential energy $U_{dr}(Z_1)$, the intrinsic fusion $B^*_{\rm fus}$ and quasifission B_{qf} barriers, quasifission rate Λ_{qf}, and the lifetime $\tau_{\rm DNS}$ of an excited DNS are calculated for the $^{12}C+^{204}Pb$, $^{19}F+^{197}Au$, $^{30}Si+^{186}W$, and $^{48}Ca+^{168}Er$ reactions which all lead to the compound nucleus ^{216}Ra.

The obtained results show that the values of fusion barrier $B^*_{\rm fus}$ are equal to zero for the more asymmetric $^{12}C+^{204}Pb$ and $^{19}F+^{197}Au$ reactions; instead, for the two other reactions, its values change slowly when the orbital angular momentum ℓ varies in the interval $0\hbar$ to $25\hbar$ due to the larger moments of inertia in massive nuclei collisions. It is also observed that the contribution of the quasifission events increases monotonically with increasing atomic number Z_1 of the lighter fragment in the DNS and the angular momentum of the compound nucleus. In conclusion, the relative stability of the DNS formed in the $^{12}C+^{204}Pb$ and $^{19}F+^{197}Au$ reactions is greater than that obtained in the $^{30}Si+^{186}W$ and $^{48}Ca+^{168}Er$ reactions.

The comparison of the results shows that the values of the quasifission rate Λ_{qf} and the DNS lifetime $\tau_{\rm DNS}$ change weakly when the angular momentum ℓ increases from around $0\hbar$ to $25\hbar$. This behavior shows very weak dependence of

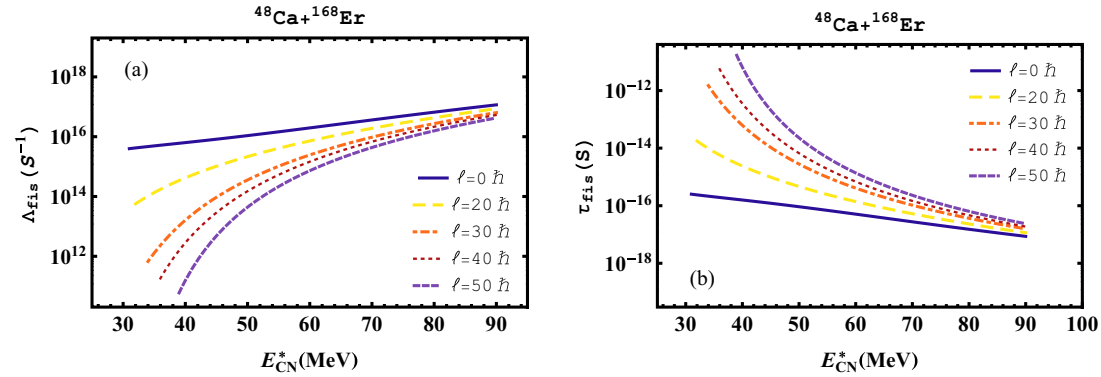

FIG. 11. The fission rate $\Lambda_{\rm fis}$ (curves from top to bottom) and the fission lifetime $\tau_{\rm fis}$ (curves from bottom to top) for the $^{48}Ca+^{168}Er$ reaction are obtained within the framework of the DNS model versus the excitation energy E^*_{CN} at the same values of angular momentum ℓ in (a) and (b), respectively.

the quasifission barrier values on ℓ in this interval. However, for higher values of ℓ ($\ell > 25\hbar$), two different behaviors are observed for the different entrance channels. It is observed that, for smaller values of E^*_{CN}, the reduction of the quasifission barrier B_{qf} is slower than the reduction of the temperature $\Theta_{\rm DNS}$ with increasing ℓ. Thus, the values of quasifission rate decrease with increasing ℓ, while the values of the DNS lifetime increase because of the increase of ℓ. On the other hand, at larger excitation energies E^*_{CN}, for the ^{30}Si + ^{186}W and ^{48}Ca + ^{168}Er reactions it can be seen that the quasifission barrier B_{qf} decreases faster than the DNS temperature $\Theta_{\rm DNS}$ with increasing ℓ. Therefore, the quasifission rate Λ_{qf} increases and, in contrast, the lifetime of the DNS decreases moderately with increasing ℓ. Moreover, the increase of E^*_{CN} leads to an increase the quasifission rate and reduces the lifetime of the DNS at a given ℓ.

It is also concluded that the DNSs corresponding to the ^{216}Ra compound nucleus through the ^{12}C + ^{204}Pb, ^{19}F + ^{197}Au, ^{30}Si + ^{186}W, and ^{48}Ca + ^{168}Er reactions behave differently at similar excitation energies. In the ^{30}Si + ^{186}W and ^{48}Ca + ^{168}Er reactions having smaller entrance channel mass asymmetry, the quasifission signature dominates over the complete fusion process. Because of the small quasifission barrier for these reactions, the lifetime of the DNS is short and its excitation energy is not sufficient to reach the saddle point. Thus, the DNS breaks down into two fragments before it transforms into the stage of the formation of a fully equilibrated compound nucleus. On the other hand, the lifetime of an excited DNS formed in these reactions is smaller than the one in the ^{12}C + ^{204}Pb and ^{19}F + ^{197}Au reaction systems. In the ^{12}C + ^{204}Pb and ^{19}F + ^{197}Au reaction systems, the quasifission signature is extremely hindered and the fused DNSs have sufficient time to reach the heavy mononuclear configuration, which equilibrates in all degrees of freedom to the compound nucleus. In other words, the dominant decay channel is complete fusion. This conclusion emphasizes the importance of the entrance channel mass asymmetry in determining the outcome of a reaction.

To understand the reaction mechanism, it is worthwhile to study the energy dependence of the fission rate and the mean lifetimes of the nuclear molecules. Therefore, for this purpose, the behaviors of the fission rate and the fission time scale are estimated for the most asymmetric ^{12}C + ^{204}Pb and also for the almost symmetric ^{48}Ca + ^{168}Er reactions. Extracted results indicate that the fission rate increases and fission lifetime decreases with increasing excitation energy E^*_{CN} at a given angular momentum. Thus, it can be seen that the survival probability of the massive compound nucleus decreases due to decrease or disappearance of the fission barrier at the large values of the excitation energy of the formed compound nucleus.

[1] W. J. Swiatecki, Phys. Scr. **24**, 113 (1981).
[2] S. Bjornholm and W. J. Swiatecki, Nucl. Phys. A **391**, 471 (1982).
[3] J. P. Blocki, H. Feldmeier, and W. J. Swiatecki, Nucl. Phys. A **459**, 145 (1986).
[4] A. C. Berriman, D. J. Hinde, M. Dasgupta, C. R. Morton, R. D. Butt, and J. O. Newton, Nature (London) **413**, 144 (2001).
[5] E. Prasad, K. M. Varier, R. G. Thomas, P. Sugathan, A. Jhingan, N. Madhavan, B. R. S. Babu, Rohit Sandal, Sunil Kalkal, S. Appannababu, J. Gehlot, K. S. Golda, S. Nath, A. M. Vinodkumar, B. P. Ajith Kumar, B. V. John, Gayatri Mohanto, M. M. Musthafa, R. Singh, A. K. Sinha, and S. Kailas, Phys. Rev. C **81**, 054608 (2010).
[6] R. Rafiei, R. G. Thomas, D. J. Hinde, M. Dasgupta, C. R. Morton, L. R. Gasques, M. L. Brown, and M. D. Rodriguez, Phys. Rev. C **77**, 024606 (2008).
[7] J. Toke, R. Bock, G. X. Dai, A. Gobbi, S. Gralla, K. D. Hildenbrand, J. Kuzminski, W. F. J. Muller, A. Olmi, H. Stelzer, B. B. Back, and S. Bjornholm, Nucl. Phys. A **440**, 327 (1985).
[8] D. J. Hinde, D. Hilscher, H. Rossner, B. Gebauer, M. Lehmann, and M. Wilpert, Phys. Rev. C **45**, 1229 (1992).
[9] W. Q. Shen, J. Albinski, A. Gobbi, S. Gralla, K. D. Hildenbrand, N. Herrmann, J. Kuzminski, W. F. J. Muller, H. Stelzer, J. Toke, B. B. Back, S. Bjornholm, and S. P. Sorensen, Phys. Rev. C **36**, 115 (1987).
[10] S. A. Karamian *et al.*, Yad. Fiz. **14**, 499 (1971).
[11] J. U. Andersen, J. Chevallier, J. S. Forster, S. A. Karamian, C. R. Vane, J. R. Beene, A. Galindo-Uribarri, J. Gomez del Campo, H. F. Krause, E. Padilla-Rodal, D. Radford, C. Broude, F. Malaguti, and A. Uguzzoni, Phys. Rev. Lett. **99**, 162502 (2007).
[12] M. Morjean, D. Jacquet, J. L. Charvet, A. L'Hoir, M. Laget, M. Parlog, A. Chbihi, M. Chevallier, C. Cohen, D. Dauvergne, R. Dayras, A. Drouart, C. Escano-Rodriguez, J. D. Frankland, R. Kirsch, P. Lautesse, L. Nalpas, C. Ray, C. Schmitt, C. Stodel, L. Tassan-Got, E. Testa, and C. Volant, Phys. Rev. Lett. **101**, 072701 (2008).
[13] J. U. Andersen, J. Chevallier, J. S. Forster, S. A. Karamian, C. R. Vane, J. R. Beene, A. Galindo-Uribarri, J. G. delCampo, C. J. Gross, H. F. Krause, E. Padilla-Rodal, D. Radford, D. Shapira, C. Broude, F. Malaguti, and A. Uguzzoni, Phys. Rev. C **78**, 064609 (2008).
[14] S. Soheyli and M. V. Khanlari, Phys. Rev. C **94**, 034615 (2016).
[15] P. Papka and C. Beck, *Clusters in Nuclei: Experimental Perspectives*, Lecture Notes in Physics, Vol. 848 (Springer, Berlin, 2012), p. 299.
[16] E. A. Cherepanov, PRAMANA J. Phys. **53**, 619 (1999).
[17] A. Nasirov, A. Fukushima, Y. Toyoshima, Y. Aritomo, A. Muminov, Sh. Kalandarov, R. Utamuratov, Nucl. Phys. A **759**, 342 (2005).
[18] G. Audi, A. H. Wapstra, and C. Thibault, Nucl. Phys. A **729**, 337 (2003).
[19] Sh. A. Kalandarov, G. G. Adamian, N. V. Antonenko, and W. Scheid, Phys. Rev. C **82**, 044603 (2010).
[20] A. Nasirov, K. Kim, G. Mandaglio, G. Giardina, A. Muminov, and Y. Kim, Eur. Phys. J. A **49**, 147 (2013).
[21] P. Fröbrich and G. R. Tillack, Nucl. Phys. A **540**, 353 (1992).
[22] W. Li, N. Wang, F. Jia, H. Xu, W. Zuo, Q. Li, E. Zhao, J. Li, and W. Scheid, J. Phys. G: Nucl. Part. Phys. **32**, 1143 (2006).

[23] H. Q. Zhang, C. L. Zhang, C. J. Lin, Z. H. Liu, F. Yang, A. K. Nasirov, G. Mandaglio, M. Manganaro, and G. Giardina, Phys. Rev. C **81**, 034611 (2010).
[24] A. V. Ignatyuk, *Statistical Properties of Excited Atomic Nuclei* (Energoatomizdat, Moscow, 1983).
[25] G. G. Adamian, N. V. Antonenko, and W. Scheid, Phys. Rev. C **68**, 034601 (2003).
[26] G. Mandaglio, G. Giardina, A. K. Nasirov, and A. Sobiczewski, Phys. Rev. C **86**, 064607 (2012).
[27] A. J. Sierk, Phys. Rev. C **33**, 2039 (1986).
[28] P. Moller and J. R. Nix, J. Phys. G: Nucl. Part. Phys. **20**, 1681 (1994).
[29] A. K. Nasirov, G. Mandaglio, G. Giardina, A. Sobiczewski, and A. I. Muminov, Phys. Rev. C **84**, 044612 (2011).
[30] A. K. Nasirov, G. Giardina, G. Mandaglio, M. Manganaro, F. Hanappe, S. Heinz, S. Hofmann, A. I. Muminov, and W. Scheid, Phys. Rev. C **79**, 024606 (2009).
[31] W. Scobel, H. H. Gutbrod, M. Blann, and A. Mignerey, Phys. Rev. C **14**, 1808 (1976).